



## OPEN ACCESS

## EDITED BY

Mohamed A. Dkhil,  
Helwan University, Egypt

## REVIEWED BY

Lamjed Mansour,  
Carthage University, Tunisia  
Rohit K. Jangra,  
LSU Health Sciences Center-Shreveport,  
United States

## \*CORRESPONDENCE

Murray E. Selkirk  
✉ m.selkirk@imperial.ac.uk

## SPECIALTY SECTION

This article was submitted to  
Molecular Cellular Parasitology,  
a section of the journal  
Frontiers in Parasitology

RECEIVED 16 October 2022

ACCEPTED 10 January 2023

PUBLISHED 26 January 2023

## CITATION

Hagen J, Ghosh S, Sarkies P and Selkirk ME  
(2023) Gene editing in the nematode  
parasite *Nippostrongylus brasiliensis* using  
extracellular vesicles to deliver active Cas9/  
guide RNA complexes.  
*Front. Parasitol.* 2:1071738.  
doi: 10.3389/fpara.2023.1071738

## COPYRIGHT

© 2023 Hagen, Ghosh, Sarkies and Selkirk.  
This is an open-access article distributed  
under the terms of the [Creative Commons  
Attribution License \(CC BY\)](#). The use,  
distribution or reproduction in other  
forums is permitted, provided the original  
author(s) and the copyright owner(s) are  
credited and that the original publication in  
this journal is cited, in accordance with  
accepted academic practice. No use,  
distribution or reproduction is permitted  
which does not comply with these terms.

# Gene editing in the nematode parasite *Nippostrongylus brasiliensis* using extracellular vesicles to deliver active Cas9/guide RNA complexes

Jana Hagen<sup>1</sup>, Subhanita Ghosh<sup>2</sup>, Peter Sarkies<sup>3</sup>  
and Murray E. Selkirk<sup>1\*</sup>

<sup>1</sup>Department of Life Sciences, Imperial College London, London, United Kingdom, <sup>2</sup>MRC London Institute of Medical Sciences, Imperial College London, London, United Kingdom, <sup>3</sup>Department of Biochemistry, University of Oxford, Oxford, United Kingdom

Despite recent advances, animal-parasitic nematodes have thus far been largely refractory to genetic manipulation. We describe here a new approach providing proof of principle that CRISPR/Cas9-mediated gene editing of parasitic nematodes is achievable using vesicular stomatitis virus glycoprotein-pseudotyped extracellular vesicles for the delivery of Cas9-single guide ribonucleoprotein complexes. We demonstrate that extracellular vesicle-delivered ribonucleoproteins can be used to disrupt a secreted deoxyribonuclease in *Nippostrongylus brasiliensis*. Introduction of a repair template encoding multiple stop codons led to measurable reduction in expression of the targeted gene. Altered transcripts corresponding to the edited locus were detected by RT-PCR, demonstrating that vesicles can access cells of tissues actively expressing the gene of interest. These data provide evidence that this technique can be employed for targeted gene editing in *N. brasiliensis*, making this species genetically tractable for the first time, although further refinement will be necessary for routine and robust interrogation of gene function.

## KEYWORDS

gene editing, CRISPR/Cas9, nippostrongylus, nematode, extracellular vesicles

## Introduction

Over a quarter of the world's population are estimated to be infected with soil-transmitted helminths, representing a severe burden of disease and disability (Jourdan et al., 2018). Additionally, gastrointestinal nematodes are responsible for major economic losses to the livestock industry, with rising multi-drug resistance to the major classes of anthelmintics (Kaplan, 2020). A major bottleneck to identifying molecules that might serve as new drug targets or vaccine candidates is the genetic intractability of most parasitic nematodes, which limits screening proteins for biological properties and essential functions.

The delivery of foreign DNA or RNA has been identified as a limiting factor for gene silencing and transgenesis in parasitic nematodes (Selkirk et al., 2012; Castelletto et al., 2020). Recently, we showed that *Nippostrongylus brasiliensis* could be transduced with vesicular stomatitis virus glycoprotein (VSV-G)-pseudotyped lentiviral particles, with entry most likely mediated by binding of VSV-G to low-density lipoprotein receptor-related (LRP) proteins (Finkelshtein et al., 2013; Hagen et al., 2021). However, the delivered expression cassette was subjected to gene silencing during worm development, such that further optimisation of the system is required in order to achieve robust and reliable transgene expression (Hagen et al., 2021).

Clustered Regularly Interspaced Short Palindromic Repeat (CRISPR)/Cas9 mediated gene editing is a powerful tool which facilitates permanent modifications in genomic DNA, and this has been successfully applied to a range of helminth species for the generation of gene knockout and knockin mutants (Gang et al., 2017; Quinzo et al., 2022). Delivery of expression cassettes or Cas9/single guide (sg)RNA ribonucleoprotein (RNP) complexes to parasitic nematodes has generally proven problematic, with two exceptions, in which a unique free-living phase (*Strongyloides*) or development of a culture system which promoted parasite development (*Brugia malayi*) facilitated genetic manipulation of parasites and selection of mutants (Gang et al., 2017; Liu et al., 2018; Liu et al., 2020).

Recently, a new approach was established for transient delivery of RNP complexes into mammalian cells using VSV-G-pseudotyped extracellular vesicles, named NanoMEDIC (nanomembrane-derived extracellular vesicles for the delivery of macromolecular cargo) (Gee et al., 2020). Proof of principle was demonstrated in several cell types which had proven difficult to transfect such as induced pluripotent stem cells, neurons and myoblasts (Gee et al., 2020). We thought that this could be a useful tool to apply to helminths, as lengthy optimisation of the viral delivery system for individual parasite species would be circumvented by production and assembly of RNP complexes in mammalian cells for which optimised expression cassettes and transfection protocols are readily available. Following the success of VSV-G-mediated uptake of lentiviral particles, we investigated whether NanoMEDIC could be utilised in *N. brasiliensis* as a model gastrointestinal nematode.

## Materials and methods

### Expression of recombinant DNase II in yeast

The coding sequence of *dnase2\_1590* was amplified from *N. brasiliensis* cDNA omitting the signal peptide and stop codon and cloned into pPICZalpha-A downstream of the coding sequence for the *Saccharomyces cerevisiae*  $\alpha$ -mating secretion factor and in frame with an N-terminal myc and 6xHis Tag. PCR was carried out using Q5 polymerase (New England Biolabs) according to manufacturer's recommendations with 500 nM of the following primers (lower case indicating nucleotides added for cloning purposes, restriction site underlined):

F-5'-aagctGAATTCGGTCTGAGTTGCAAGAACATGGAGG-3'

R-5'-tttggTCTAGAGCGGTTTTGTTTGTCTTCTTGCTCG-3'

Following transformation of *Pichia pastoris* X-33, protein expression was optimised for single colonies and scaled up following the EasySelect *Pichia* expression protocol (Invitrogen). His-tagged proteins were purified from yeast supernatants by nickel chelating chromatography and protein concentration determined by Bradford assay.

### Antibody production, protein preparation and western blotting

A polyclonal antiserum to *N. brasiliensis* recombinant DNase II was raised by subcutaneous immunisation of a rat with 100  $\mu$ g protein emulsified in alum, followed by 3 boosts of 50  $\mu$ g protein *via* the same route at weeks 4, 6 and 8, and the animal bled at week 9. Parasite proteins were prepared from larval and adult parasites by homogenising in phosphate buffered saline, 0.25 mM n-dodecyl- $\beta$ -D-maltoside and protease inhibitors for somatic extracts, whereas secreted proteins were collected by *in vitro* culture in serum-free RPMI-1640 plus antibiotics and concentrated in vivaspin concentrators with a 3 kDa cutoff, as previously described (Huang et al., 2010). Western blotting was performed *via* standard procedures following resolution of 5  $\mu$ g parasite proteins by SDS-12% polyacrylamide gel electrophoresis and blotting to polyvinylidene difluoride membrane. Rat anti-DNase II was used at 1:500 dilution, rabbit anti-rat IgG-horseradish peroxidase (Sigma) used as secondary antibody and the blot visualised using enhanced chemiluminescence western blotting detection reagents (Amersham Bioscience).

### Vector construction

For facilitated cloning of synthesised sgRNA oligos, a *NheI* restriction site was introduced into the RGR expression vector (pL-5LTR-RGR(DMD#1)-AmCyan-A, Addgene plasmid #138482). To do this, the entire sequence between two *SpeI* restriction sites flanking the RGR region was amplified by PCR adding an *NheI* and *AvrII* restriction site to the 3' end and used to replace the original sequence *via* *SpeI* and *AvrII* to allow for cloning of gRNA coding regions *via* *KpnI* and *NheI*. PCR was carried out in 50  $\mu$ l reactions using Q5 polymerase (New England Biolabs) according to manufacturer's recommendations with 1 ng of the RGR plasmid as template and 500 nM of the following primers (lower case indicating nucleotides added for cloning purposes and restriction site underlined): F-5'-GCTTGCATGCCGACATGGATTATTGACTAGTCCC-3'; R-5'-attgaCCTAGGGCTAGCTCTAGAGCGGCCGTCCCATTCGCCATGC-3.

The CRISPR/Cas-derived RNA-guided endonucleases (RGEN) algorithm was used to predict *Streptococcus pyogenes* (Sp) Cas9 gRNA targets with a 5'-NGG-3' Protospacer Adjacent Motif (PAM) in exon 3 of the *dnase-2* gene and subsequent off-target screening against the *N. brasiliensis* genome. Oligonucleotides encoding gRNAs for subsequent integration into the RGR plasmid *via* *KpnI* and *NheI* were synthesised (GeneArt, Thermo Fisher Scientific) with the following structure: 5'-*KpnI*-inverted first 6 nt of the guide RNA-HH ribozyme-guide RNA-gRNA scaffold-HDV ribozyme-*NheI*-3' (complete sequence Supplementary Figure 3). Plasmids were

maintained in NEB stable *Escherichia coli* (New England Biolabs). Positive transformants were selected on LB agar plates containing 50  $\mu\text{g ml}^{-1}$  ampicillin. Constructs were verified for error-free integration of transgenes by routine Sanger sequencing (Eurofins Genomics).

## Extracellular vesicle production

NanoMEDIC were produced in HEK293T cells maintained in Dulbecco's Modified Eagle's Medium (DMEM) at 37°C, 10% foetal calf serum (FCS), 2 mM L-glutamine, 100 units  $\text{ml}^{-1}$  penicillin and 100  $\mu\text{g ml}^{-1}$  streptomycin, as described previously (Gee et al., 2020) with some modifications. In brief, per well of a 6-well plate,  $3 \times 10^6$  cells were transfected with 1.25  $\mu\text{g}$  of gRNA-encoding plasmid, 1.25  $\mu\text{g}$  of pHLS-EF1a-FRB-SpCas9-A (Addgene plasmid #138477), 1.25  $\mu\text{g}$  of pHLS-EF1a-FKBP12-Gag<sup>HIV</sup> (Addgene plasmid #138476), 250 ng of pcDNA1-Tat<sup>HIV</sup> (Addgene plasmid #138478) and 500 ng of pMD2.G (VSV-G) (Addgene plasmid #12259), using Lipofectamine 2000 at a ratio of 1:2.5 (Life Technologies). After 16 hours, the transfection medium was replaced with 2 ml of reduced serum culture medium (5% FCS) supplemented with 300  $\mu\text{M}$  A/C heterodimerization agent (formerly AP21967, Takara Bio), 20 mM HEPES and 10  $\mu\text{M}$  cholesterol (balanced with methyl- $\beta$ -cyclodextrin, Sigma) (Chen et al., 2009). VSV-G-EVs were produced in HEK293T cells following transfection of  $3 \times 10^6$  cells with 1.25  $\mu\text{g}$  of pMD2.G per well of a 6-well plate with Lipofectamine 2000 at a ratio of 1:2.5. The cell culture supernatant was changed after 18 hours as for NanoMEDIC, omitting the heterodimerisation agent. After an additional incubation of 48 hours at 37°C and 10% CO<sub>2</sub>, the EV-containing cell supernatant was harvested, centrifuged at 2,000  $\times g$  for 20 min at 4°C and passed through a 0.45  $\mu\text{m}$  Acrodisc syringe filter. NanoMEDIC and VSV-G-EVs were generally concentrated using 10 kDa vivaspins columns and washed twice with serum-free growth medium (NanoMEDIC) or trehalose buffer (10% trehalose in PBS) (VSV-G-EVs). Following centrifugation at 4,000  $\times g$  for 15 min at 4°C, the flow-through was discarded and EVs gently resuspended in 2 ml of the respective buffer before aliquoting into cryovials and storage at -80°C. For enrichment by polymer-based precipitation, 4 ml of Lenti-X concentrator (Takara Bio) was added to 12 ml of cell supernatant and the mixture incubated at 4°C with gentle agitation for 18 hours. Precipitated EVs were then pelleted by centrifugation at 3,000  $\times g$  for 45 min and 4°C and resuspended in 2 ml of trehalose buffer.

## Analysis of extracellular vesicles

The composition of EVs was analysed by Western blot and Nano-flow cytometry. Western blotting was performed *via* standard procedures following resolution of 12  $\mu\text{l}$  concentrated EV preparations by SDS-12% polyacrylamide gel electrophoresis under reducing (Cas9, VSV-G) or non-reducing (CD63, CD81) conditions. Primary antibodies were used at 1:1000 dilution: mouse anti-human CD63 (clone H5C6, Biolegend); mouse anti-human CD81 (TAPA-1)

(clone 5A6, Biolegend); rabbit anti-VSV-G (Covance); mouse anti-CRISPR (Cas9) (clone 7A9, Biolegend).

Concentrated NanoMEDIC preparations were analysed for their nanoparticle content by nano-flow cytometry using a NanoAnalyzer calibrated against trehalose buffer. Before acquisition, samples were diluted 1:100 and 1:200 in trehalose buffer. The concentration of particles with diameters larger than 100 nm was determined following gating using the NanoFCM<sup>TM</sup> Silica Nanospheres Cocktail (S16M-Exo, diameter:68~155 nm) as a standard.

## Loading of extracellular vesicles with homology directed repair templates

Oligonucleotides encoding the HDR templates (Supplementary Figure 3) were synthesized (Invitrogen) and reconstituted in nuclease-free water at a concentration of 1  $\mu\text{g } \mu\text{l}^{-1}$ . VSV-G-EVs were then loaded with ssDNA as described previously (Lamichhane et al., 2015). In brief, 5  $\mu\text{g}$  of ssDNA were added to 95  $\mu\text{l}$  of VSV-G-EVs in trehalose buffer and EVs then transferred to a 1 mm electroporation cuvette (BioRad) placed on ice. EVs were electroporated by exponential decay with two pulses at 400 V and 125  $\mu\text{F}$  using a GenePulser Xcell electroporator (Bio-Rad). Cuvettes were placed on ice immediately after electroporation and incubated on ice for 20 min. EVs were then transferred to fresh microfuge tubes and the cuvette washed with one volume (100  $\mu\text{l}$ ) of RPMI and added to the tube. To alleviate aggregation, EDTA was added to a final concentration of 1 mM and EVs incubated at room temperature for 15 min, gently resuspended several times during incubation (Lamichhane et al., 2015).

## Parasite infection, recovery and exposure to extracellular vesicles

*N. brasiliensis* were maintained in male SD rats, and infective larvae isolated from faecal cultures using a Baermann apparatus. Larvae were activated to feed as previously described (Huang et al., 2010) for 48 to 72 hrs in RPMI1640, 0.65% glucose, 2 mM L-glutamine, 100 U  $\text{ml}^{-1}$  penicillin, 100  $\mu\text{g ml}^{-1}$  streptomycin, 100  $\mu\text{g ml}^{-1}$  gentamicin, 20 mM HEPES, 2% rat serum (worm culture medium), then washed twice in serum-free medium prior to exposure to EVs. Per well of a 12-well plate, approximately 3,000 - 4,000 activated L3 were exposed to 200  $\mu\text{l}$  NanoMEDIC and/or 200  $\mu\text{l}$  of VSV-G-EVs, volumes adjusted to 1 ml with serum-free medium and 10  $\mu\text{g ml}^{-1}$  polybrene (Sigma) and 200  $\mu\text{g ml}^{-1}$  gentamicin added. EV preparations in control worms were substituted with HEK293T cell supernatant from untransfected cells. Following incubation for 18 to 24 hrs, worms were transferred to a 15 ml tube and washed twice in 10 ml of warm serum-free worm medium containing 1 mM EDTA with centrifugation at 150  $\times g$  for 1 min between washes. Worms were then resuspended in 2 ml complete worm medium (or serum-free medium when testing for ES products) and incubated for another 24 to 48 hours at 37°C, 5% CO<sub>2</sub>.

## Detection of homology directed repair in genomic DNA

Homology directed repair (HDR) was effected utilising a single stranded oligodeoxynucleotide with ~50 nt homology arms, which introduced a series of 6 stop codons following a single (sgRNA91) or double (sgRNA46 and 91) stranded DNA break. Detection of HDR was performed by PCR analysis of genomic DNA following exposure of activated L3 to NanoMEDIC with or without the addition of HDR-containing EVs. Worms were washed twice in 10 ml of PBS at 37°C, 72 hrs post exposure to EVs, and genomic DNA isolated using the DNeasy Blood and Tissue DNA extraction kit (Qiagen). PCR was performed using Q5 polymerase with an annealing/extension temperature of 72°C. Primer pairs were designed to amplify fragments from the adjacent exon (2 or 4) and the HDR region (6xstop). The following primers were used with resultant fragment sizes indicative of editing. Exon 2 forward primer (5'-GATTCGGCTATTGGTGCAACTGTAAAGC-3') and 6xstop reverse primer (5'-ATCCCCGTGCTACTCAGTTACCTAGTACTTA-3') gave rise to a 240 bp fragment with a single stranded DNA break (sgRNA91) and a 200 bp fragment with a double stranded DNA break (sgRNA46 and 91). The 6xstop forward primer (TAAGTGACTAGGTAAGTACTGAGTAGC-3') and exon 4 reverse primer (5'-TCGAGCCTGATTCGGGGTAGTCG-3') gave rise to a 165 bp fragment in both cases. Exon 3 forward primer (5'-ACCTCAAATTGCCTACAACGAC-3') and 6xstop reverse primer gave rise to a 125 bp fragment with a single stranded DNA break (sgRNA91) and an 85 bp fragment with a double stranded DNA break (sgRNA46 and 91). PCR was also performed with primers specific to exon 3 flanking the HDR integration site: exon 3 forward primer as indicated above and exon 3 reverse primer (5'-GGAATCTTGGCACACTGTGTACCAGC-3'). Amplification of *eif-3c* (eukaryotic translation initiation factor 3 subunit C) was performed to control for genomic DNA integrity (forward primer 5'-GAACACGTTGTAGCTGCGTCA-3' and reverse primer 5'-AATAGGTTCTCAGCGATTCCGTT-3').

## Preparation of DNA libraries and deep sequencing

PCR was performed using Q5 polymerase with an annealing/extension temperature of 72°C using exon 3 forward (5'-ACCTCAAATTGCCTACAACGAC-3') and reverse (5'-GGAATCTTGGCACACTGTGTACCAGC-3') primer to amplify the WT allele and the edited allele, and the product was purified using gel extraction. DNA libraries for deep sequencing were made using the NEBNext Ultra II DNA library preparation kit (New England Biolabs) according to the manufacturer's instructions. Sequencing was performed by the London Institute of Medical Sciences Genomics facility. Reads were mapped to the predicted PCR products from wild type and edited alleles using Bowtie2 (Langmead and Salzberg, 2012). SNPs and indels were mapped using samtools mPileup (Li et al., 2009). We then used Varscan2 (Koboldt et al., 2012) using the commands pileup2snp and pileup2indel to identify putative SNPs and indels respectively, requiring a minimum average quality of 20 and setting a minimum

frequency of 1 in 10000 to enable low frequency alterations to be detected. Data were read into R using the read.table function and comparison of the different files enabled SNPs that were present in the untransfected control to be identified and removed as likely sequencing errors or PCR artefacts. Line plots indicating the frequency of SNPs at each position divided by total reads aligned to that position were constructed to illustrate the distribution of mutations along the template.

## Reverse transcription PCR and Real-Time quantitative PCR

Total RNA was extracted using TRIreagent (Sigma) and converted to cDNA using an iScript cDNA kit (Biorad) following removal of contaminating genomic DNA by DNase I. Reverse Transcription PCR (RT-PCR) was carried out using Q5 DNA polymerase (New England Biolabs) according to the manufacturer's recommendations. An edited *dnase2* transcript was confirmed with an exon 2-specific forward primer (5'-GATTCGGCTATTGGTGCAACTGTAAAGC-3') and a reverse primer binding the 6xSTOP region in the HDR template (5'-ATCCCCGTGCTACTCAGTTACCTAGTACTTA-3'), resulting in a product of approximately 140 bp. RT-PCR amplification of *eif-3c* was performed to control for RNA integrity (forward primer 5'-GAACACGTTGTAGCTGCGTCA-3' and reverse primer 5'-AATAGGTTCTCAGCGATTCCGTT-3').

Real-Time quantitative PCR (RT-qPCR) was carried out with a Step-One PLUS Fast Real-time PCR cycler (Applied Biosystems) under standard fast cycling conditions using PowerUP SYBR Green PCR Master Mix (Applied Biosystems) and 250 nM target gene specific forward and reverse primers. PCR amplification efficiencies were established for each primer pair (Pfaffl, 2001) and ranged between 1.9 and 2.1. Cycle threshold (Ct) values of target genes were normalised to the geometric mean of *eif-3C* (NBR\_0001150401; eukaryotic translation initiation factor 3 subunit C) and *idhg-1* (NBR\_0000658601; isocitrate dehydrogenase gamma) (Hagen et al., 2021) and calibrated to the mean untreated control (wild type) samples for relative quantification by the comparative Ct method (Livak and Schmittgen, 2001). The primers were (forward (F), reverse (R)): *Nb-nuc-1* F: 5'-TGACGAACCATAACAACGGCA-3', R: 5'-TGGAACACTGTGGATCAGCC-3'; *eif-3C* F: 5'-GAACACGTTGTAGCTGCGTCA-3', R: 5'-AATAGGTTCTCAGCGATTCCGTT-3'; *idhg-1* F: 5'-CAGAAATTGGGAGACGGCCT-3', R: 5'-CCGAGAAACCAGCTGCATAGA-3'; *dnase2\_1590\_E6F*: 5'-TGGAAACTTGGAGAAACGGTGCTG-3'; *dnase2\_1590\_E7R*: 5'-ACATCTCCGATACAACTAGGGGCTCC-3'.

## Deoxyribonuclease activity assay

Supernatant collected from worms cultured in serum-free medium was thawed and all reactions prepared on ice. Per test sample, 500 ng of a plasmid DNA substrate in 10 µl nuclease free water was placed in PCR tubes and a 10 µl droplet of worm supernatant transferred to the side of the tube. Reactions were initiated by centrifugation and samples placed immediately into a

PCR cycler pre-warmed to 37°C and incubated for 2 to 10 min. After heat inactivation at 75°C for 10 min, 4 µl of agarose loading dye was added and 10 µl of the sample separated on a 1% agarose gel.

To assess the dynamics of DNase secretion by L3, worms were extensively washed in serum-free medium, counted and resuspended at 2500 L3 ml<sup>-1</sup>. Per time point tested, 80 µl of worm suspension (200 L3) was added to 20 µl of plasmid DNA solution (2 µg in 20 µl RPMI). Following incubation for 15, 30, 60 or 120 min at 37°C, 5% CO<sub>2</sub>, 80 µl of supernatant was carefully aspirated and transferred to a PCR tube. Samples were immediately frozen at -20°C. For analysis, tubes were placed directly from the freezer into a PCR cycler prewarmed to 75°C and heat inactivated for 10 min. Loading dye was added and the samples separated on a 1% agarose gel.

## Statistics

Treatment groups were analysed for significant differences with the Kruskal-Wallis test and Dunn's *post-hoc* test in relation to the control group. Values are expressed as the median with range or the mean ± SEM, and significant differences were determined using GraphPad Prism. P values of <0.05 were considered significant, \*p<0.05.

## Results

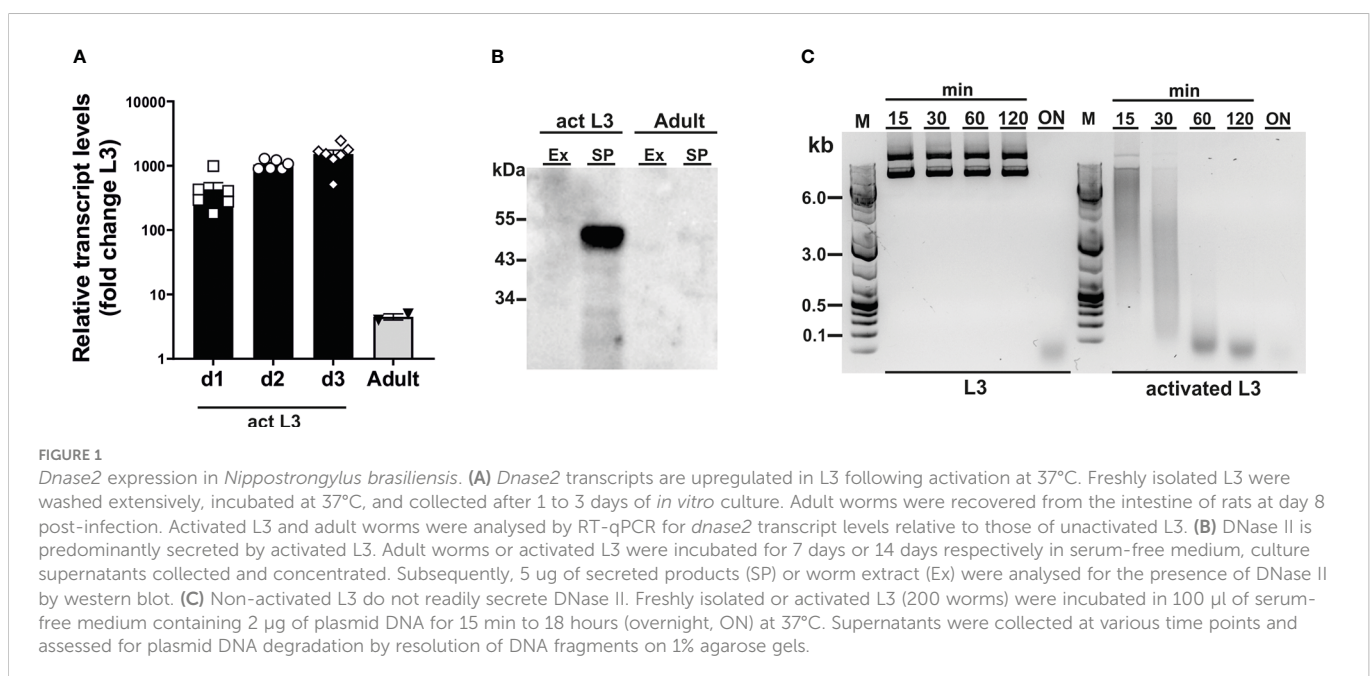
### Characterisation of *dnase2* expression in different life cycle stages

To assess susceptibility of CRISPR-mediated gene editing in *N. brasiliensis*, we chose secreted DNase II as a target gene (Bouchery et al., 2020), as endonuclease activity in secreted products provides a means for functional analysis of gene expression. While the DNase II has been described to be secreted from infective larvae (Sotillo et al.,

2014), a profile of expression in different stages has not been determined. Because a shift in temperature to 37°C acts as a cue for exsheathment and initiation of feeding in infective larvae (L3) (Huang et al., 2010), we first analysed levels of DNase II transcripts and secretion of active enzyme in L3 prior to and during activation by culture at 37°C in the presence of rat serum. Incubation at the elevated temperature led to a sharp increase in DNase II transcripts relative to those of unactivated L3, i.e. isolated directly from faecal cultures in a state of diapause, peaking at an approximate 1000-fold increase after 2-3 days (Figure 1A). Transcript levels were drastically reduced in adult worms compared with activated L3, but remained approximately 5-fold above those in non-activated L3 (Figure 1A). Western blot analysis of parasite secreted products confirmed that the DNase II was released predominantly by activated L3 (Figure 1B). Given the detection of low levels of DNase II transcripts in non-activated L3, there was a possibility that the protein might be pre-synthesised and stored in secretory vesicles allowing for immediate release upon entering the host. To assess this, we exposed non-activated and activated L3 to plasmid DNA during culture at 37°C. However, non-activated L3 did not secrete sufficient amounts of DNase II for effective degradation of DNA within the first 2 hours of incubation at 37°C, although complete degradation was achieved following overnight incubation (Figure 1C). In contrast, degradation of DNA in the culture supernatant was observed immediately following exposure to previously activated L3.

### Generation of extracellular vesicles containing DNase II-ribonucleoprotein complexes or a single stranded oligodeoxynucleotide

The genomic DNA sequence of DNase II was identified in NBR\_scaffold\_0001590 following alignment of the published cDNA sequence (GenBank: M938457) (Bouchery et al., 2020) to the genomic



*N. brasiliensis* database PRJEB511 available on WormBase ParaSite. Nine exons were defined. Exon 3 and exon 7 both encode HxK motifs; this is characteristic of DNase II as the two motifs are required to form the active site (Schafer et al., 2007) (Figure 2A). Notably, while the corresponding amino acid sequence derived from NBR\_scaffold\_0001590 and M938457 was mainly conserved, some differences were detected in the cDNA sequences which could affect the prediction of effective sgRNAs (Supplementary Figures 1A, B). Expression of NB\_Dnase2\_1590 was confirmed in our laboratory strain of *N. brasiliensis* following cloning of the cDNA sequence into a

yeast expression vector and subsequent sequencing such that sgRNA design was based on NB\_Dnase2\_1590.

For transient delivery of Cas9/gRNA complexes, we adapted a recently developed NanoMEDIC approach established in mammalian cells using VSV-G-pseudotyped extracellular vesicles (Gee et al., 2020). To predict sgRNA target sequences, the Cas-Designer (RGEN) algorithm was used, which allows for off-target screening against the *N. brasiliensis* genome (Bae et al., 2014a; Park et al., 2015). We chose exon 3 as a target region as it encodes one of the two HxK motifs of functional DNases (Schafer et al., 2007) (Figure 2A). While

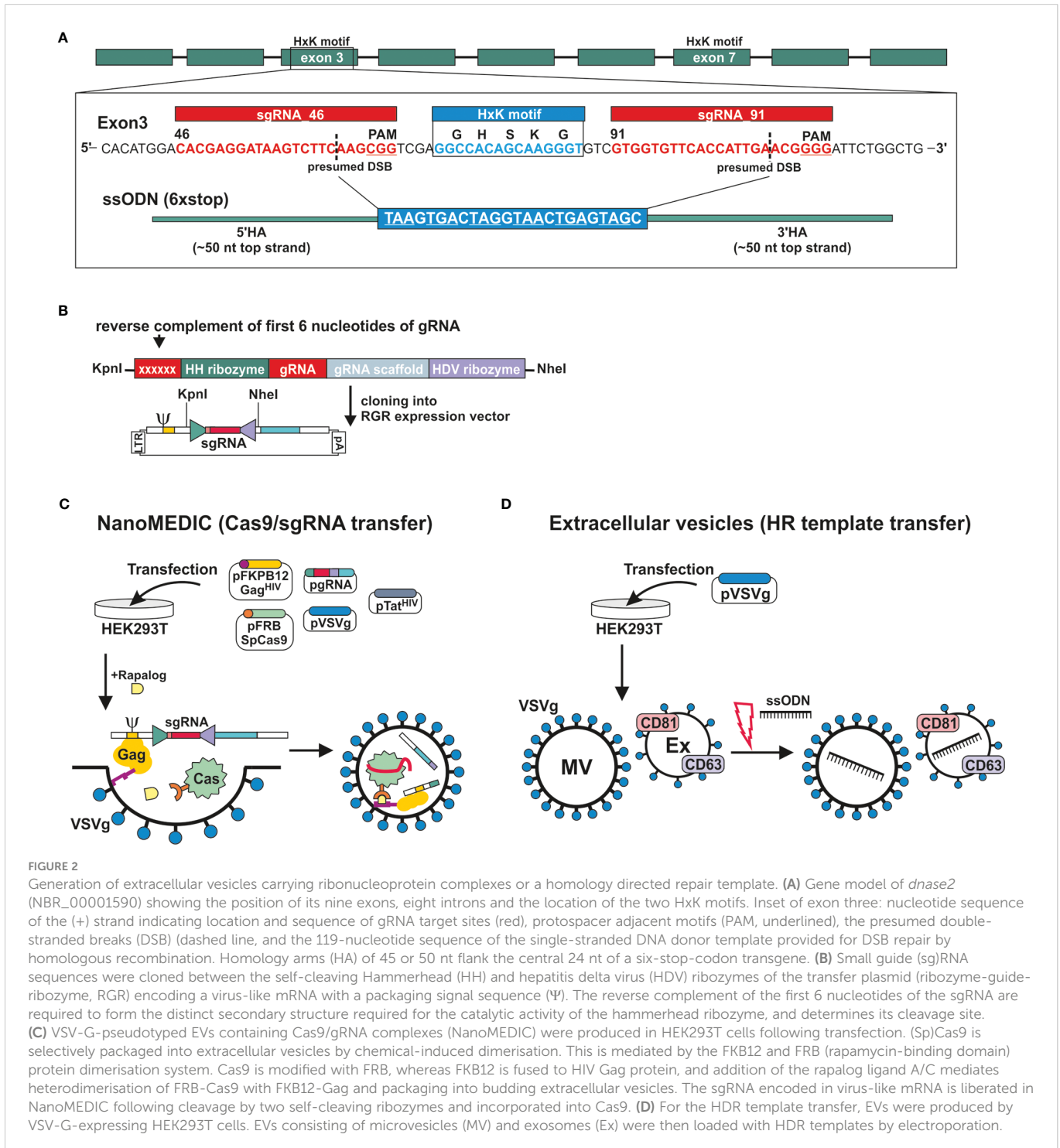


FIGURE 2

Generation of extracellular vesicles carrying ribonucleoprotein complexes or a homology directed repair template. (A) Gene model of *dnase2* (NBR\_00001590) showing the position of its nine exons, eight introns and the location of the two HxK motifs. Inset of exon three: nucleotide sequence of the (+) strand indicating location and sequence of gRNA target sites (red), protospacer adjacent motifs (PAM, underlined), the presumed double-stranded breaks (DSB) (dashed line), and the 119-nucleotide sequence of the single-stranded DNA donor template provided for DSB repair by homologous recombination. Homology arms (HA) of 45 or 50 nt flank the central 24 nt of a six-stop-codon transgene. (B) Small guide (sg)RNA sequences were cloned between the self-cleaving Hammerhead (HH) and hepatitis delta virus (HDV) ribozymes of the transfer plasmid (ribozyme-guide-ribozyme, RGR) encoding a virus-like mRNA with a packaging signal sequence (Ψ). The reverse complement of the first 6 nucleotides of the sgRNA are required to form the distinct secondary structure required for the catalytic activity of the hammerhead ribozyme, and determines its cleavage site. (C) VSV-G-pseudotyped EVs containing Cas9/gRNA complexes (NanoMEDIC) were produced in HEK293T cells following transfection. (Sp)Cas9 is selectively packaged into extracellular vesicles by chemical-induced dimerisation. This is mediated by the FKB12 and FRB (rapamycin-binding domain) protein dimerisation system. Cas9 is modified with FRB, whereas FKB12 is fused to HIV Gag protein, and addition of the rapalog ligand A/C mediates heterodimerisation of FRB-Cas9 with FKB12-Gag and packaging into budding extracellular vesicles. The sgRNA encoded in virus-like mRNA is liberated in NanoMEDIC following cleavage by two self-cleaving ribozymes and incorporated into Cas9. (D) For the HDR template transfer, EVs were produced by VSV-G-expressing HEK293T cells. EVs consisting of microvesicles (MV) and exosomes (Ex) were then loaded with HDR templates by electroporation.

some gRNAs were predicted that covered the HxK region, these did not achieve a frameshift prediction score over 66, which is recommended in order to minimise the possibility of unwanted in-frame deletions (Bae et al., 2014b). The two highest scoring gRNAs, guide 46 and 91, flanking the HxK motif in exon 3, were cloned between the self-cleaving Hammerhead (HH) and hepatitis delta virus (HDV) ribozymes of the transfer plasmid (ribozyme-guide-ribozyme, RGR) (Figure 2B). If the deletion was insufficient or frameshift not achievable using either guide, then the EV approach would allow for multiplexing to include both guide RNAs deleting the entire HxK motif coding sequence. Corresponding VSV-G-pseudotyped EVs containing RNP complexes (NanoMEDIC) were produced in HEK293T cells following transfection with the RGR and four packaging plasmids encoding Cas9, Gag, VSV-G and Tat (Figure 2C) (Gee et al., 2020).

The NanoMEDIC delivery system utilises two distinct homing mechanisms to recruit Cas9 and a sgRNA into extracellular vesicles in HEK293 producer cells. *Streptococcus pyogenes* (Sp)Cas9 is selectively packaged into extracellular vesicles by chemical-induced dimerisation. This is mediated by the FKB12 and FRB (rapamycin-binding domain) protein dimerisation system (Putyrski and Schultz, 2012). Cas9 is modified with FRB, whereas FKB12 is fused to HIV Gag protein, and addition of the rapalog (rapamycin analogue) ligand A/C mediates heterodimerisation of FRB-Cas9 with FKB12-Gag and packaging into budding extracellular vesicles. Long terminal repeat (LTR)-driven transcription of the RGR transfer plasmid produces a virus-like mRNA encoding the sgRNA and containing a packaging signal sequence ( $\Psi$ , Figure 2B) which directs RNA incorporation into budding vesicles. The sgRNA encoded in virus-like mRNA is liberated in NanoMEDIC by self-cleavage of the flanking ribozymes. Dissociation of the complexes occurs after dilution of the A/C heterodimerizer once the vesicles fuse with recipient cell membranes, in this case those of *N. brasiliensis*.

To test whether homology directed repair (HDR) could be achieved following induction of double strand breaks, we generated a single-strand oligonucleotide (ssODN) template encoding a series of 6 stop codons interspaced by single nucleotides to allow for all possible open reading frames and ~50 nt homology arms (Figure 2A), as previously described (Ittiprasert et al., 2019). The introduction of premature stop codons allows for degradation of modified transcripts by nonsense-mediated decay and/or premature termination of translation (Hug et al., 2016). Overexpression of VSV-G in HEK293T cells leads to an increased production of VSV-G-expressing EVs, termed 'gesicles', that can be utilised for transfer of membrane, cytoplasmic and nuclear proteins (Mangeot et al., 2011). We therefore loaded VSV-G-pseudotyped EVs with the ssODN template and tested whether they could be transferred to *N. brasiliensis* L3 (Figure 2D) (Lamichhane et al., 2015; Meyer et al., 2017).

## NanoMEDIC in conjunction with an extracellular vesicle-delivered homology directed repair template induces site directed mutagenesis in *Nippostrongylus* infective larvae

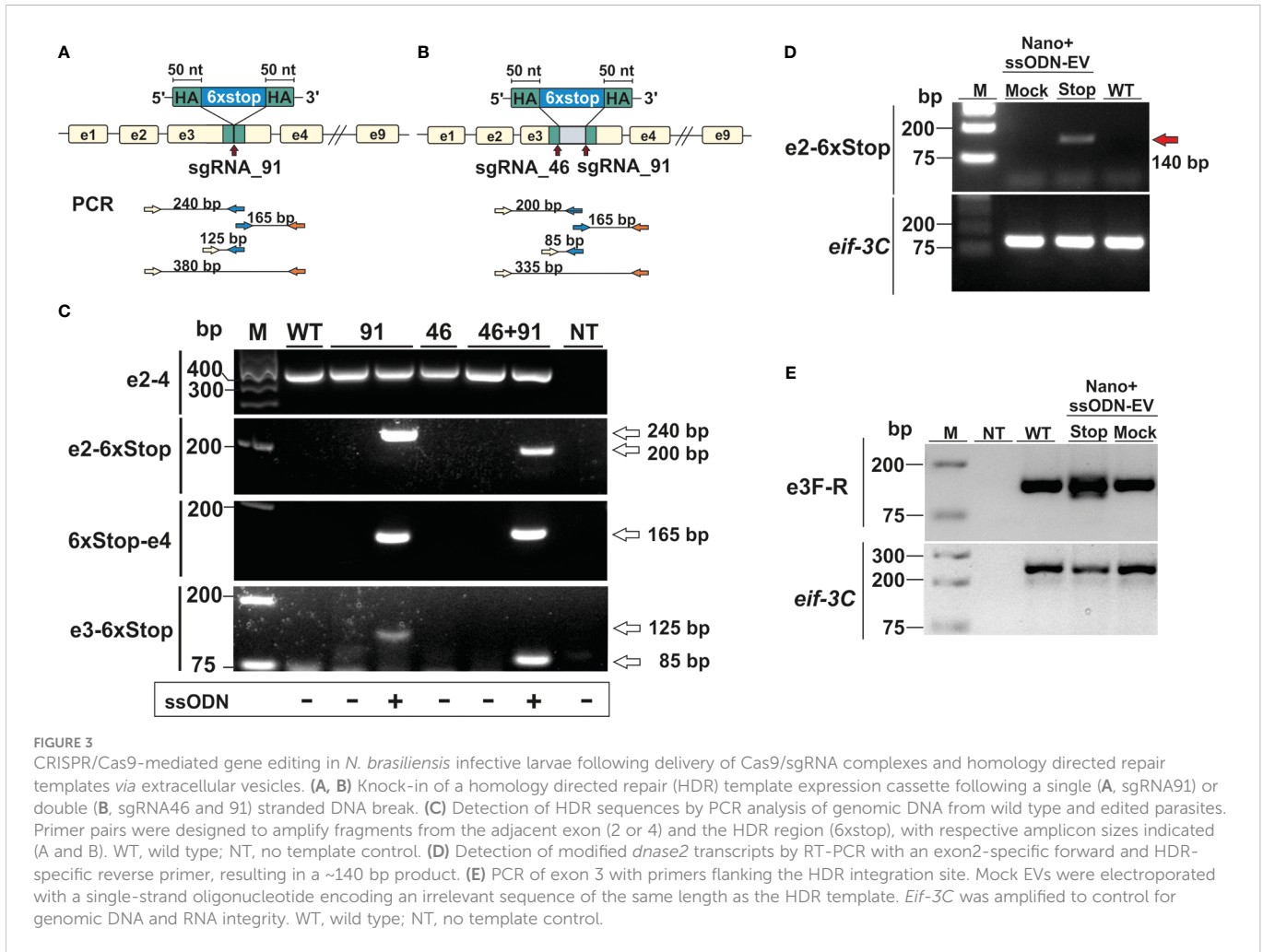
In our first series of experiments, activated L3 were exposed to NanoMEDIC containing sgRNAs binding at nucleotide 46 and/or 91

of exon 3 in the presence or absence of EVs containing the STOP\_ssODN for HDR. Parasite genomic DNA was then assessed by PCR for modifications introduced by HDR (Figures 3A, B). PCR with primers binding the stop codon region and adjacent exon 2 or 4 led to amplification of expected PCR products (Figure 3C), indicating that NanoMEDIC in conjunction with EV-delivered ssODN templates could be used for site directed mutagenesis in *N. brasiliensis*. Furthermore, the presence of modified *dnase2* transcripts was confirmed by RT-PCR with an exon 2-specific forward primer and a reverse primer binding the 6xSTOP region, resulting in a product of approximately 140 bp (Figure 3D). PCR from genomic DNA with the same primer pair produced an amplicon of approximately 200 bp (Figure 3C). Importantly, the presence of modified cDNA provided evidence that NanoMEDIC and EV-delivered ssODN can reach tissues actively expressing DNase II following ingestion.

## Non-homologous end joining does not lead to effective mutations in infective larvae

In previous studies with *Strongyloides stercoralis*, non-homologous end joining (NHEJ) of CRISPR/Cas9-induced double-strand breaks following microinjection of RNP complexes into the gonad resulted in large deletions, while smaller insertions or deletions (indels) appeared to be absent. Similarly, PCR of genomic DNA carried out with an exon 2-binding forward and an exon 4-binding reverse primer resulted in a single fragment of ~350 bp in all samples tested, which could not resolve possible indels (Figure 3C). To compensate for the possibility that deletions were insufficient, or frameshift not achievable using either guide, further experiments were carried out using a combination of both guide RNAs, with or without the addition of a ssODN allowing for deletion of the entire motif. To facilitate detection of smaller changes, a further PCR was carried out with primers flanking the double stranded break sites of exon 3 (Figure 3E). While multiple PCR fragments were generated in the NanoMEDIC + 6xSTOP\_ssODN sample indicating integration of the HDR template, PCR with exon 3-binding forward and reverse primers still failed to resolve possible indels in worms exposed to NanoMEDIC (Figure 3E).

To examine potential low frequency errors induced by CRISPR/Cas9-mediated editing, we performed deep sequencing of PCR products derived from worms transfected with CRISPR/Cas9 either with or without the repair template. In worms transfected with CRISPR/Cas9 alone, after removing potential sequencing errors and PCR artefacts (see methods) single nucleotide polymorphisms (SNPs) at low frequency were detected mapping to the wild type allele of the DNase II gene, indicating that the enzyme could introduce breaks triggering error prone repair (Figure 4A). Interestingly, addition of the repair template led to an altered pattern of mutations in the wild type allele, without changing the frequency (Figure 4B). Similar patterns were seen for small indels mapping to the wild type allele (Figures 4C, D). However, the total frequency of SNPs and indels mapping to the edited allele was extremely low and similar to the frequency of mutations mapping to the wild type allele (Figures 4E, F), confirming that the homology directed repair was mostly accurate.



### Diminished DNase activity in CRISPR/Cas9 mutated larvae

We next assessed whether modifications introduced into the DNase II gene resulted in measurable reduction of secreted enzyme. Reduced DNase activity was observed in supernatants collected for 3 days following exposure of activated L3 to NanoMEDIC and ssODN (Figure 5A). While complete degradation of donor DNA was observed 5 min after exposure to supernatant from control worms, this required longer (10 min) incubation with supernatant of worms exposed to NanoMEDIC and the STOP\_ssODN. Delayed DNA degradation was only observed following delivery of the STOP\_ssODN via VSV-G-EVs (ssODN-EV), while direct electroporation of NanoMEDIC with the STOP\_ssODN (Nano+ssODN) was unsuccessful. Reduced nuclease activity was also not observed in supernatants from worms exposed to NanoMEDIC and Mock-EVs electroporated with a ssODN encoding an irrelevant sequence of the same length as the HDR template.

To assess the timeframe of delayed DNA degradation by modified worms, secreted products were assessed for their nuclease activity by adding a substrate plasmid DNA to the culture medium alongside the worms and following degradation over time (Figure 5B). No intact DNA was detected after 30 min, and complete degradation recorded 60 min after culture with worms exposed to ssODN-EVs only. In

contrast, co-culture of NanoMEDIC-exposed worms revealed the presence of some intact plasmid DNA after 30 min. This was more pronounced when worms were exposed to NanoMEDIC + ssODN-EVs, with some larger DNA fragments still present 60 min after co-culture (Figure 2B). Furthermore, RT-qPCR revealed a reduction in *dnase2* transcript levels by ~25% (mean log<sub>2</sub> ± SEM = -0.45 ± 0.12) in NanoMEDIC + ssODN-EV samples, compared to the ssODN-EV only group (-0.003 ± 0.09) (p=0.048, Kruskal-Wallis test with Dunn's post-hoc; Figure 5C), indicating nonsense-mediated decay of modified transcripts. No significant decrease of *dnase2* transcripts (-0.17 ± 0.09) was recorded in the NanoMEDIC-only group (p=0.74). These data, together with PCR analysis of genomic DNA, indicate that the majority of NanoMEDIC-induced gene disruption can be repaired by non-homologous end joining, and that editing is enhanced by homology-directed repair.

Because *N. brasiliensis* DNase II has been demonstrated to degrade neutrophil extracellular traps, it has been suggested to facilitate migration of L3 through the skin and lung tissues of their mammalian host (Bouchery et al., 2020). The moderate silencing of the *dnase2* gene achieved in this study did not lead to a reduction in worm numbers in the intestines of infected mice (Figure 5D). Nevertheless, these data provide proof of principle that CRISPR/Cas9-induced gene editing can be achieved in infective larvae of *N. brasiliensis* by harnessing extracellular vesicle-mediated delivery of

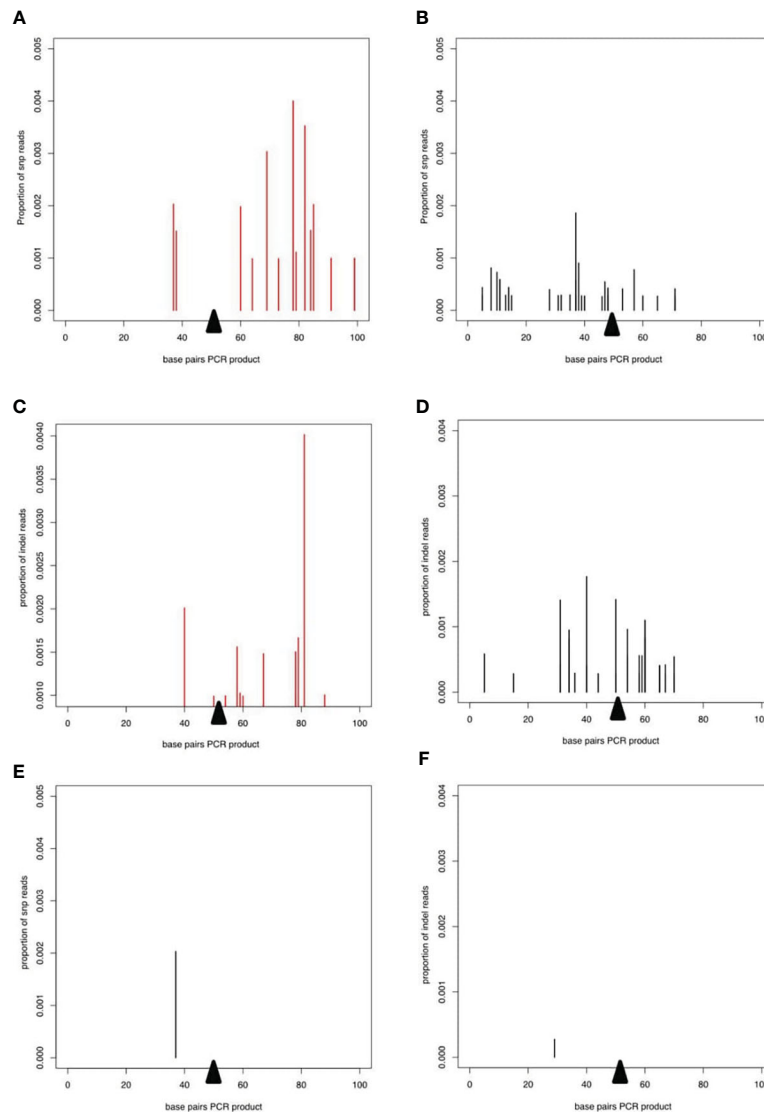


FIGURE 4

Deep sequencing of PCR product from worms transfected with CRISPR/Cas9 guide RNA complexes. In all plots, the proportion of reads corresponding to SNPs or indels is shown on the y axis and the presumed breakpoint is indicated by a black triangle. (A, B) SNPs on the WT allele after transfection with the CRISPR/Cas9 guide RNA complex without (A) or with (B) the repair template. (C) and (D) Indels on the WT allele for CRISPR/Cas9 guide RNA complex without (C, D) the repair template. (E) SNPs and (F) indels mapping to the repair template after transfection with the CRISPR/Cas9 guide RNA complex and the repair template.

RNPs and HDR templates, providing a new route for genetic manipulation of parasitic nematodes.

## Expression of a NUC-1 orthologue by *Nippostrongylus brasiliensis*

As reduction of secreted DNase II activity did not result in altered recovery of adult worms from infected mice, we hypothesised that additional DNase II activities may be encoded in the parasite genome providing some degree of redundancy. A search of WormBase ParaSite revealed that NBR\_0000088201 encoded an orthologue of lysosomal DNase II from *Caenorhabditis elegans* termed NUC-1 (Hedgecock et al., 1983; Wu et al., 2000). The predicted amino acid sequence is shown in Figure 6A, aligned with that of the *N. brasiliensis*

secreted DNase II (NBR\_00001590) (Bouchery et al., 2020) and *C. elegans* NUC-1, revealing 65% identity between the mature *N. brasiliensis* and *C. elegans* NUC-1 proteins. Examination of transcript levels by real-time RT-PCR (qPCR) revealed that *Nb\_nuc-1* is expressed at fairly constant levels through to adult worms (Figure 6B). Transcript levels for the secreted DNase II were 10-fold higher than *Nb\_nuc-1* in activated L3, and at least 10-fold lower than *Nb\_nuc-1* in resting L3 and adult worms (Figure 6C). This suggests that *Nb\_nuc-1* has more of a housekeeping role, consistent with a lysosomal function, and it is notable that no nuclease activity was detected in culture supernatants of L3 within the first 2 hours following activation (Figure 1C) despite appreciable levels of *Nb\_nuc-1* transcripts. In contrast, expression of the secreted DNase II was almost exclusively associated with larval activation, suggesting that this is the major or sole enzyme released into the mammalian host

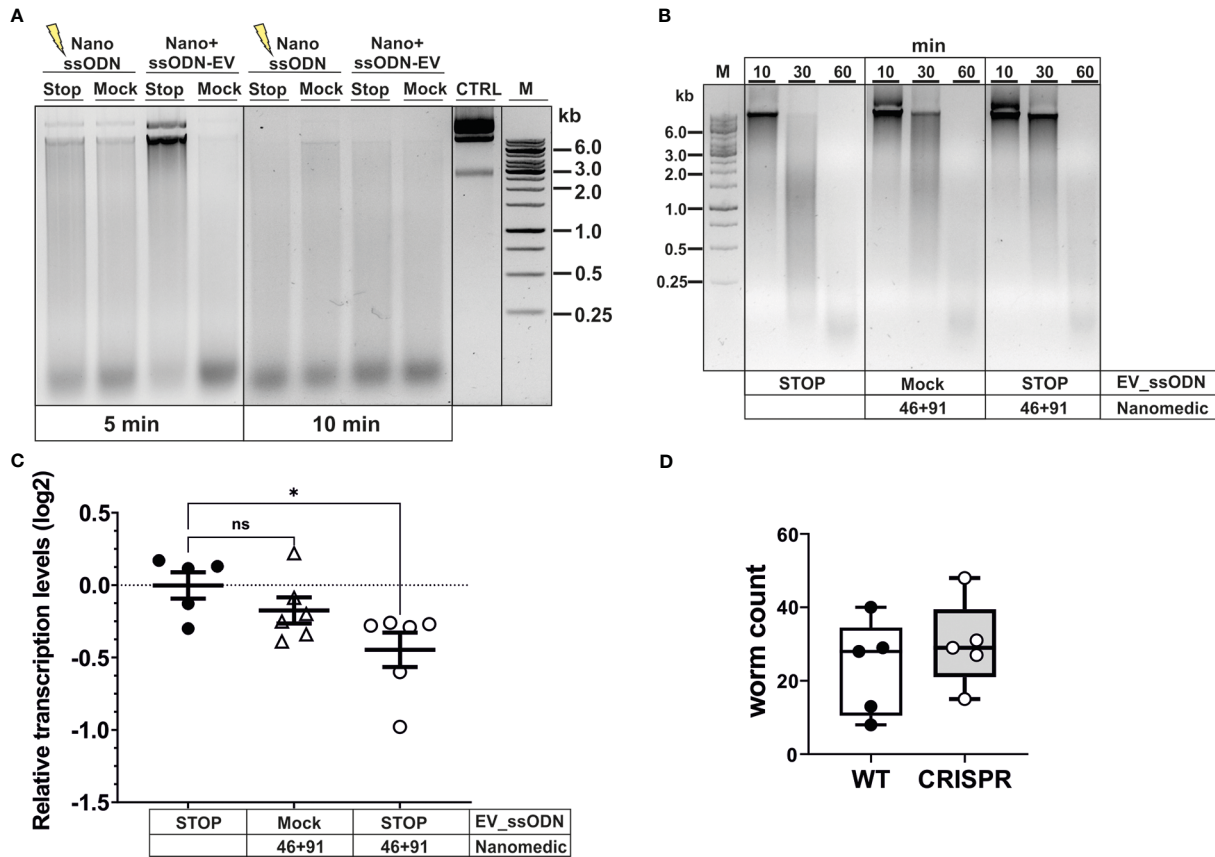


**FIGURE 5**  
 Editing of *dnase2* results in reduced enzyme activity in larval secreted products. **(A)** Reduced DNase activity in larval secreted products. Activated L3 were exposed to EVs for 18 hours, washed and incubated for a further 48 hours. The HDR template was either electroporated into NanoMEDIC (NanosODN) or VSV-G-pseudotyped EVs (ssODN-EV). Mock EVs were electroporated with a ssODN encoding an irrelevant sequence of the same length as the HDR template. Larval secreted products were collected and assessed for DNase activity as described in Materials and methods. Undigested plasmid DNA (CTRL) was resolved on gels with test samples. **(B)** Time course of delayed DNA degradation by secreted products from modified worms. Activated L3 were exposed to EVs for 18 hours then incubated with plasmid DNA for 10, 30 or 60 min and supernatants analysed for DNA degradation by gel electrophoresis. **(C)** Downregulation of secreted *dnase2* transcripts in activated L3s after exposure to EVs. Transcript levels were assessed by RT-qPCR three days after transduction relative to wild type control larvae and normalised against the geometric mean of Ct values of reference genes *eif-3C* and *idhg-1*. Scatter plot with the mean ± sem of data from 2 independent experiments with 3 biological replicates each consisting of ~2,000 larvae. Treatment groups were analysed for significant differences with the Kruskal-Wallis test and Dunns *post-hoc* test in relation to the wild type. \*Statistical significance:  $p < 0.05$ . ns, not significant. **(D)** Reduction of DNase II secretion did not lead to lower parasite recovery in mice. Activated L3 were exposed to EVs for 18 hrs, washed and used to infect BALB/c mice. Adult worms were recovered from the intestines at day 5 post-infection and counted.

and primarily responsible for degradation of extracellular/environmental DNA in the early stages of infection.

## Discussion

Nanoparticles, including EVs, have become an important tool for delivery of cargo including drugs, proteins, and nucleic acids to mammalian cells both *in vitro* and *in vivo*. EVs released by cells include microvesicles, exosomes, and apoptotic bodies, which differ in their biogenesis and size. However, while EVs have been described in secreted products of many helminths and suggested to be involved in signalling to the host (Drurey and Maizels, 2021), utilisation as vehicles to deliver functional cargo to the parasites remains unexplored.

Here, we demonstrate that CRISPR/Cas9-mediated gene editing of *N. brasiliensis* is achievable using VSV-G-pseudotyped EVs (NanoMEDIC) for the delivery of RNP complexes. NanoMEDIC

induced DNA double strand breaks, and homology directed repair was achieved through simultaneous delivery of a ssODN template *via* VSV-G-pseudotyped EVs (Figure 1B). Edited transcripts were detected by RT-PCR, demonstrating that EVs can access cells of tissues actively expressing the gene of interest. Furthermore, gene disruption and the introduction of a repair template encoding 6 stop codons led to measurable reduction of target gene expression (*dnase2*), demonstrating that the technique can be employed for the identification and characterisation of molecules in parasites involved in disease processes. Deep sequencing of PCR products from populations of edited worms and alignment to the predicted edited locus (which would have identical sequence to the recombination cassette) or to the wild type locus indicated that almost all the reads which mapped to the edited allele did so perfectly (Figure 4). This means that the process of insertion that occurs during CRISPR targeting must have a very high accuracy, i.e. it almost always inserts an exact copy of the repair template rather than one with a mutation in it.

**A**

```

DNaseII_1590  ---MWTIFLIIPAIVGNVDAGLSCKNMEGKDVDWFAAVKLPNSVDERK-----GRTFA      50
Ce_NUC-1     MGLSPA AVLIFLLLGVSQTYAAFSCKDQSGNDVDWFAVYKMPIEKDDGSVTGLAGGVAWY      60
Nb_NUC-1     -----MIILLFLLFSPFVFSCKDQNNNDVDWFAVYKMPVESADNSIPGIQSGTGWY      53
              :::::  ..  .:::***: ..:*****. *: * : : . * :

DNaseII_1590  YYDSTQNGWK-FSPLPINSTDSAIGATVKQLYSDNSYHL-KIAYNDHDPHG-----      100
Ce_NUC-1     YVDVNKKGLTLP SAKTLDNDQAIAYTLQQYYDKQNDKTI FHV MYNDE-PWGSKSTSGIK      119
Nb_NUC-1     YVDSNKKGALLPSTKTL DATQAIAYTLNQYYSKKSNDTI FHL MYNDE-PYNGTSSLM--      110
              * * ::* * * : : . * . * . * . * . * . * . * . * . * . * . * . * .

DNaseII_1590  -----HEDKSSSGFGHSGKGVVVFETIERGFVLVHVSVP RFPDPEKYDY PESG      145
Ce_NUC-1     LEEILSNRVYSNYTHEDDSTSTAFGH TKGTIEFDGTSGVWLVHVS VPLFPNPTKYEY PVS G      179
Nb_NUC-1     -DMLSS-----NRVRATVQFEGHTKGTMEFDNKSGIWL IHSVPKFP PPNSSYSYPTSG      160
              . : : * : * : * : * : * : * : * : * : * : * : * : * : * : * : * :

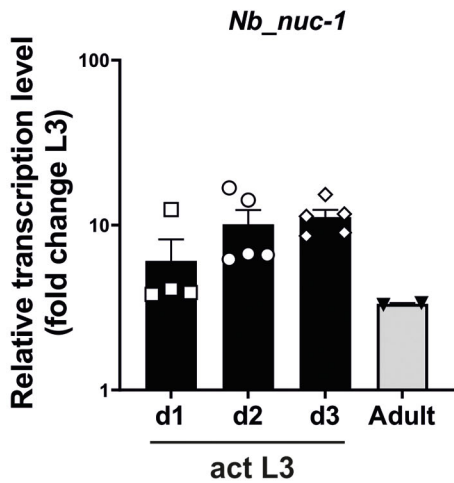
DNaseII_1590  SKFAQSFICLTLSSDFLPDISQYLRYSQVTPFVMNLPENHKLLAPYLVDVQAKKSLGRAD      205
Ce_NUC-1     HDYGQTMCLMCFKYAQLKSI GTQLFFNRPN IYSSNLP TNMAADNADLAKAIAGQ--YQKG      237
Nb_NUC-1     HDYGQTMWCLSFYPYSQLGNIATQLYFNKPD IYSSALPTSMASEYPTLAKVVAGK--YQQG      218
              : : * : * : * : * : * : * : * : * : * : * : * : * : * : * : * :

DNaseII_1590  TKFTSTHSYQTMGGKRFTILAKHKKFDNDLWHDFIALYFKTPMAVETWRNGAAKNVGTQC      265
Ce_NUC-1     QPFQSVIELETMAGYSFTNF AKSKEFNADLYDTLVAPTLKTDLVVETWRRGSEI--PLDC      295
Nb_NUC-1     EPHSSVITLTTSGGASFLSFAKTNEFNNDLYDGLVAPTLKADLIAETWRRGSEV--PLSC      276
              . * . * * * * : * : * : * : * : * : * : * : * : * : * : * : * :

DNaseII_1590  GVGYNVYDITQVKIL-DKVNSSKDHSKNGVSMEEERPLVCIGD VNRQESQFKRGGGAVC      324
Ce_NUC-1     KLTYHANDALSIHVGSTTAFSYTKDHSKMAHSADMTKPWVCIGD INRMTSQYVRGGGTTC      355
Nb_NUC-1     SQTYHTNDALTVKVGTTTEFKYTKDHSKMAVSTDATKPWVCIGD INRMTSQYVRGGGTTC      336
              * : * * : : : : * : * : * : * : * : * : * : * : * : * : * : * :

DNaseII_1590  MEDEKLWNTFHDSVKS YLNCGEVQERKNKDEDNKTESKPKKPSKKTNKT      373
Ce_NUC-1     ISSSFLWKAYSVI-ATQNNCA-----      375
Nb_NUC-1     LSSSFLWKAFNVI-KTENTC-----      355
              : . . * : * : : : : *
    
```

**B**



**C**

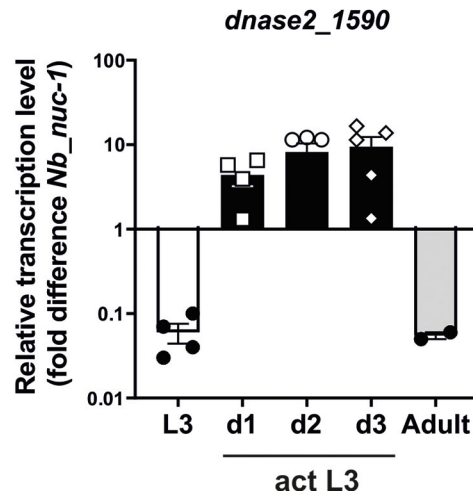


**FIGURE 6** Detection of a *nuc-1* orthologue in *Nippostrongylus brasiliensis*. **(A)** Amino acid sequence of Nb\_NUC-1 (NBR\_0000088201) inferred by orthology to *C. elegans* NUC-1. Signal peptide cleavage site (blue arrow) and HKD motifs are indicated (red border). **(B)** *Nb\_nuc-1* is upregulated in L3 following activation at 37°C. Transcript levels are shown relative to unactivated L3. **(C)** *Dnase2\_1590* transcript levels relative to *Nb\_nuc-1* in different life cycle stages and culture of L3 at 37°C up to 3 days. Interleaved scatter plot with bars and mean ± sem of 2 independent experiments with 2-3 biological replicates. \* indicates identity of amino acids in alignment.

As in previous studies with *Strongyloides stercoralis* (Gang et al., 2017), in the absence of a HDR template we could not detect smaller insertions or deletions following NHEJ. However, large genetic deletions of up to 500 bp in length following NHEJ have been described in *S. stercoralis* (Gang et al., 2017) and *Schistosoma mansoni* (Sankaranarayanan et al., 2020). Due to the PCR design in our study, with primers spanning exon 2 to exon 4 of the DNase II

gene, the presence of larger deletions cannot be excluded. However, detection of large deletions by whole genome sequencing may be challenging, as targeting tissues with direct access to EVs will result in mosaic genomes. The high abundance of wild type alleles masking edited genes has also been an issue in *S. stercoralis* (Gang et al., 2017). While not reaching significance in our readouts so far, some reduction in transcript and DNase activity was observed in the

absence of HDR, such that optimisation of NanoMEDIC production and purity may lead to improved gene disruption by NHEJ. However, consistent with previous studies in other species (Gang et al., 2017; Ittiprasert et al., 2019), gene disruption is more effective when HDR is employed, and it facilitates detection of edited genes by providing unique primer binding sites. Interestingly, while a ssODN template was sufficient to achieve HDR in *N. brasiliensis* L3 in this study, a double stranded DNA template was necessary for repair in *S. stercoralis* following injection of the gonad (Gang et al., 2017). This may be indicative of different repair mechanisms in somatic and germline cells, as previously described in *C. elegans* (van Schendel et al., 2015).

Direct injection into the gonad has the advantage of potentially generating homozygous offspring, whereas NanoMEDIC targets tissues with direct access to EVs. The EVs used in this study are similar in size to lentiviral particles (~150-200 nm) and possess a cell membrane-derived envelope expressing VSV-G. Lentiviral particles can access cells in the intestine of *N. brasiliensis* L3, and interference with expression of secreted acetylcholinesterases suggests that they can also access subventral glands (Hagen et al., 2021). This is important, as it suggests that NanoMEDIC may be utilised for targeting tissues expressing secreted proteins, as shown here for the DNase II. The same study showed that lentiviral particles can gain access to the germline, as integrated viral genomes were evident in a small proportion of the F1 generation (Hagen et al., 2021). The route to the germline is unclear, and further studies are required to determine whether this is similarly possible with NanoMEDIC. If so, then this introduces the possibility of generating stable homozygous gene-edited parasite lines, which may be necessary for robust interrogation of gene function.

Although we have shown that *N. brasiliensis* could be transduced with lentivirus, the transgene expression cassettes were subject to epigenetic silencing, and RNAi could not be maintained following development to adult stages (Hagen et al., 2021). CRISPR/Cas9-mediated gene editing offers a means to circumvent these problems, as more stable expression should be possible by site-directed integration of transgenes into regions less prone to epigenetic silencing. Lentiviral delivery of a Cas9 expression cassette has been superseded in *S. mansoni* by lipofection of *in vitro* assembled RNP complexes and simultaneous delivery of an HDR template by electroporation (Ittiprasert et al., 2019). Furthermore, RNP complexes outperformed plasmid DNA-encoded Cas9 expression cassettes in *Strongyloides* (Gang et al., 2017). Unlike *Strongyloides*, most parasitic nematodes do not have a free-living phase to facilitate microinjection. Using EVs for delivery of pre-assembled RNP complexes (Montagna et al., 2018; Campbell et al., 2019; Mangeot et al., 2019; Gee et al., 2020) and HDR templates (Lamichhane et al., 2015) thus offers an alternative to techniques employed thus far, and pseudotyping EVs with VSV-G allows for receptor-mediated uptake similar to viral transduction (Montagna et al., 2018; Campbell et al., 2019; Mangeot et al., 2019; Gee et al., 2020).

Due to their short half-life, RNPs are rapidly degraded, resulting in precise site-directed editing with low off-target frequencies (Vakulskas and Behlke, 2019). Another major advantage is that RNPs are produced and assembled in mammalian cell lines for which optimised expression systems are readily available, avoiding lengthy optimisation of Cas9 expression

cassettes for expression in the respective parasite. Use of mammalian cell lines facilitates cost effective, large scale production of EVs. Furthermore, in contrast to other vesicular delivery approaches relying on stochastic uptake of RNPs (Mangeot et al., 2019) or fusion of SpCas9 to Gag (van Schendel et al., 2015), NanoMEDIC utilise the Gag and FRB-FKB12 homing system to actively incorporate RNPs into budding EVs, and contain an average of 7 Cas9 molecules per vesicle (Gee et al., 2020). Moreover, VSV-G and Gag actively mediate the release of EVs from cells resulting in average titres of approximately  $1 \times 10^{10}$  particles per ml in our studies (Supplementary Figure S2).

Further optimisation of preparation and delivery of EVs will be necessary to improve editing efficiencies. Nanoflow analysis showed that NanoMEDIC preparations contained up to 90% exosomes (Supplementary Figure S2). Concentration in spin columns resulted in slightly less exosome (vesicles <100 nm) content than polymer-based precipitation (Supplementary Figure S2). NanoMEDIC have an average size of ~150 nm, and DNA is predominantly taken up by microvesicles (~150 nm) on electroporation (Lamichhane et al., 2015). The high content of exosomes is likely to saturate available receptors and impair effective uptake by NanoMEDIC. Polymer-based precipitation results in large quantities of lipids which may compete with available LDL receptors. Improved purity may thus require affinity chromatography (Gee et al., 2020) or a combination of filter columns (Brennan et al., 2020).

In addition to loss of gene function by gene disruption, CRISPR/Cas9 provides a means to integrate foreign genes and expression cassettes *via* HDR (Chu et al., 2015). Introduction of a traceable reporter or tag would allow sorting or enrichment of mutant larvae, which would aid in generating stable edited parasite lines. It would also help to define the limitations of the EV delivery system in terms of which tissues can be accessed and manipulated, and facilitate investigation of gene expression patterns. For such studies, targeting a constitutively expressed, common gene such as tubulin, might be more effective. Introduction of a reporter would require delivery of a dsDNA donor. Utilisation of a dsDNA template might allow editing in a wider range of tissues and improve HDR efficiencies as dsDNA templates usually have longer homology arms. Delivery of dsDNA *via* EVs is limited by their loading capacity, with an optimal length of DNA up to 750 bp but not exceeding 1000 bp (Lamichhane et al., 2015), although loading capacities might be improved through optimisation of electroporation conditions (Lamichhane et al., 2015; Lennaard et al., 2021).

In summary, we have demonstrated that EVs can be utilised as a vehicle to deliver functional cargo to a parasitic nematode and achieve CRISPR/Cas9-mediated gene editing. Although the methodology clearly needs further development and optimisation in order to rigorously interrogate gene function, it provides a new route for genetic manipulation of this important group of pathogens and should be applicable to a wide range of species.

## Data availability statement

The data presented in the study are deposited in the NCBI SRA (Sequence Read Archive) repository, accession number PRJNA907367.

## Ethics statement

The animal study was reviewed and approved by Animal Welfare Ethical Review Board at Imperial College London.

## Author contributions

Conceived and designed the experiments: JH, MS, PS. Performed the experiments: JH, SG, MS, PS. Analyzed the data: JH, PS, MS. Wrote the paper: JH, MS, PS. All authors contributed to the article and approved the submitted version.

## Funding

This study was funded by a BBSRC grant to MES, PS and JH (BB/S001085/1).

## Conflict of interest

The authors declare that the research was conducted in the absence of any commercial or financial relationships that could be construed as a potential conflict of interest.

## Publisher's note

All claims expressed in this article are solely those of the authors and do not necessarily represent those of their affiliated organizations,

## References

- Bae, S., Kweon, J., Kim, H. S., and Kim, J. S. (2014b). Microhomology-based choice of Cas9 nuclease target sites. *Nat. Methods* 11 (7), 705–706. doi: 10.1038/nmeth.3015
- Bae, S., Park, J., and Kim, J. S. (2014a). Cas-OFFinder: a fast and versatile algorithm that searches for potential off-target sites of Cas9 RNA-guided endonucleases. *Bioinformatics* 30 (10), 1473–1475. doi: 10.1093/bioinformatics/btu048
- Bouchery, T., Moyat, M., Sotillo, J., Silverstein, S., Volpe, B., Coakley, G., et al. (2020). Hookworms evade host immunity by secreting a deoxyribonuclease to degrade neutrophil extracellular traps. *Cell Host Microbe* 27 (2), 277–289 e276. doi: 10.1016/j.chom.2020.01.011
- Brennan, K., Martin, K., FitzGerald, S. P., O'Sullivan, J., Wu, Y., Blanco, A., et al. (2020). A comparison of methods for the isolation and separation of extracellular vesicles from protein and lipid particles in human serum. *Sci. Rep.* 10 (1), 1039. doi: 10.1038/s41598-020-57497-7
- Campbell, L. A., Coke, L. M., Richie, C. T., Fortuno, L. V., Park, A. Y., and Harvey, B. K. (2019). Gesicle-mediated delivery of CRISPR/Cas9 ribonucleoprotein complex for inactivating the HIV provirus. *Mol. Ther.* 27 (1), 151–163. doi: 10.1016/j.yjth.2018.10.002
- Castelletto, M. L., Gang, S. S., and Hallem, E. A. (2020). Recent advances in functional genomics for parasitic nematodes of mammals. *J. Exp. Biol.* 223 (Pt Suppl 1), 1–11. doi: 10.1242/jeb.206482
- Chen, Y., Ott, C. J., Townsend, K., Subbiah, P., Aiyar, A., and Miller, W. M. (2009). Cholesterol supplementation during production increases the infectivity of retroviral and lentiviral vectors pseudotyped with the vesicular stomatitis virus glycoprotein (VSV-G). *Biochem. Eng. J.* 44 (2-3), 199–207. doi: 10.1016/j.bej.2008.12.004
- Chu, V. T., Weber, T., Wefers, B., Wurst, W., Sander, S., Rajewsky, K., et al. (2015). Increasing the efficiency of homology-directed repair for CRISPR-Cas9-induced precise gene editing in mammalian cells. *Nat. Biotechnol.* 33 (5), 543–548. doi: 10.1038/nbt.3198
- Drurey, C., and Maizels, R. M. (2021). Helminth extracellular vesicles: Interactions with the host immune system. *Mol. Immunol.* 137, 124–133. doi: 10.1016/j.molimm.2021.06.017
- Finkelshtein, D., Werman, A., Novick, D., Barak, S., and Rubinstein, M. (2013). LDL receptor and its family members serve as the cellular receptors for vesicular stomatitis virus. *Proc. Natl. Acad. Sci. U.S.A.* 110 (18), 7306–7311. doi: 10.1073/pnas.1214441110
- Gang, S. S., Castelletto, M. L., Bryant, A. S., Yang, E., Mancuso, N., Lopez, J. B., et al. (2017). Targeted mutagenesis in a human-parasitic nematode. *PLoS Pathog.* 13 (10), e1006675. doi: 10.1371/journal.ppat.1006675
- Gee, P., Lung, M. S. Y., Okuzaki, Y., Sasakawa, N., Iguchi, T., Makita, Y., et al. (2020). Extracellular nanovesicles for packaging of CRISPR-Cas9 protein and sgRNA to induce therapeutic exon skipping. *Nat. Commun.* 11 (1), 1334. doi: 10.1038/s41467-020-14957-y
- Hagen, J., Sarkies, P., and Selkirk, M. E. (2021). Lentiviral transduction facilitates RNA interference in the nematode parasite *Nippostrongylus brasiliensis*. *PLoS Pathog.* 17 (1), e1009286. doi: 10.1371/journal.ppat.1009286
- Hedgecock, E. M., Sulston, J. E., and Thomson, J. N. (1983). Mutations affecting programmed cell deaths in the nematode *Caenorhabditis elegans*. *Science* 220 (4603), 1277–1279. doi: 10.1126/science.6857247
- Huang, S. C., Chan, D. T., Smyth, D. J., Ball, G., Gounaris, K., and Selkirk, M. E. (2010). Activation of *Nippostrongylus brasiliensis* infective larvae is regulated by a pathway distinct from the hookworm *Ancylostoma caninum*. *Int. J. Parasitol.* 40 (14), 1619–1628. doi: 10.1016/j.ijpara.2010.06.004
- Hug, N., Longman, D., and Caceres, J. F. (2016). Mechanism and regulation of the nonsense-mediated decay pathway. *Nucleic Acids Res.* 44 (4), 1483–1495. doi: 10.1093/nar/gkw010
- Ittiprasert, W., Mann, V. H., Karinshak, S. E., Coghlan, A., Rinaldi, G., Sankaranarayanan, G., et al. (2019). Programmed genome editing of the omega-1 ribonuclease of the blood fluke, *Schistosoma mansoni*. *Elife* 8, e41337. doi: 10.7554/eLife.41337

or those of the publisher, the editors and the reviewers. Any product that may be evaluated in this article, or claim that may be made by its manufacturer, is not guaranteed or endorsed by the publisher.

## Supplementary material

The Supplementary Material for this article can be found online at: <https://www.frontiersin.org/articles/10.3389/fpara.2023.1071738/full#supplementary-material>

### SUPPLEMENTARY FIGURE 1

Alignment of cDNA and derived amino acid sequences for MN938457.1 (GenBank) and NBR\_00001590 (Wormbase ParaSite). (A) cDNA sequence alignment. (B) Derived amino acid sequence alignment

### SUPPLEMENTARY FIGURE 2

Analysis of extracellular vesicle preparations. (A) Analysis of extracellular vesicle production by western blot. Extracellular vesicles (EV) or NanoMEDIC (Nano-containing cell supernatants) were concentrated using vivaspin columns (VIVA) or precipitation with Lenti-X concentrator (LX) as described in Materials and methods. Western blotting was performed following SDS-PAGE under reducing conditions to determine the presence of Cas9 and VSV-G, or under non-reducing conditions for the presence of CD63 and CD81. (B) Analysis by Nano-flow cytometry. NanoMEDIC preparations concentrated by ultrafiltration (VIVAspin) or precipitation (Lenti-X) were analysed for their nanoparticle content by nano-flow cytometry as described in Materials and methods. The table shows the concentration and proportion of particles with diameters larger than 100 nm.

### SUPPLEMENTARY FIGURE 3

Guide RNA-encoding region synthesised for cloning into RGR plasmid and ssODN sequences for homology directed repair. Key: Red: guide RNA target sequence; Yellow: reverse complement of first 6 nucleotides of target; Blue: Hammerhead ribozyme; Green: Hepatitis Delta virus ribozyme; Lower case: restriction endonuclease sites.

- Jourdan, P. M., Lamberton, P. H. L., Fenwick, A., and Addiss, D. G. (2018). Soil-transmitted helminth infections. *Lancet* 391 (10117), 252–265. doi: 10.1016/S0140-6736(17)31930-X
- Kaplan, R. M. (2020). Biology, epidemiology, diagnosis, and management of anthelmintic resistance in gastrointestinal nematodes of livestock. *Vet. Clin. North Am. Food Anim. Pract.* 36 (1), 17–30. doi: 10.1016/j.cvfa.2019.12.001
- Koboldt, D. C., Zhang, Q., Larson, D. E., Shen, D., McLellan, M. D., Lin, L., et al. (2012). VarScan 2: somatic mutation and copy number alteration discovery in cancer by exome sequencing. *Genome Res.* 22 (3), 568–576. doi: 10.1101/gr.129684.111
- Lamichhane, T. N., Raiker, R. S., and Jay, S. M. (2015). Exogenous DNA loading into extracellular vesicles via electroporation is size-dependent and enables limited gene delivery. *Mol. Pharm.* 12 (10), 3650–3657. doi: 10.1021/acs.molpharmaceut.5b00364
- Langmead, B., and Salzberg, S. L. (2012). Fast gapped-read alignment with bowtie 2. *Nat. Methods* 9 (4), 357–359. doi: 10.1038/nmeth.1923
- Lennaard, A. J., Mamand, D. R., Wiklander, R. J., El Andaloussi, S., and Wiklander, O. P. B. (2021). Optimised electroporation for loading of extracellular vesicles with doxorubicin. *Pharmaceutics* 14 (1), 38. doi: 10.3390/pharmaceutics14010038
- Li, H., Handsaker, B., Wysoker, A., Fennell, T., Ruan, J., Homer, N., et al. (2009). The sequence alignment/map format and SAMtools. *Bioinformatics* 25 (16), 2078–2079. doi: 10.1093/bioinformatics/btp352
- Liu, C., Grote, A., Ghedin, E., and Unnasch, T. R. (2020). CRISPR-mediated transfection of *Brugia malayi*. *PLoS Negl. Trop. Dis.* 14 (8), e0008627. doi: 10.1371/journal.pntd.0008627
- Liu, C., Mhashilkar, A. S., Chabanon, J., Xu, S., Lustigman, S., Adams, J. H., et al. (2018). Development of a toolkit for piggyBac-mediated integrative transfection of the human filarial parasite *Brugia malayi*. *PLoS Negl. Trop. Dis.* 12 (5), e0006509. doi: 10.1371/journal.pntd.0006509
- Livak, K. J., and Schmittgen, T. D. (2001). Analysis of relative gene expression data using real-time quantitative PCR and the 2(-delta delta C(T)) method. *Methods* 25 (4), 402–408. doi: 10.1006/meth.2001.1262
- Mangeot, P. E., Dollet, S., Girard, M., Ciancia, C., Joly, S., Peschanski, M., et al. (2011). Protein transfer into human cells by VSV-g-induced nanovesicles. *Mol. Ther.* 19 (9), 1656–1666. doi: 10.1038/mt.2011.138
- Mangeot, P. E., Risson, V., Fusil, F., Marnef, A., Laurent, E., Blin, J., et al. (2019). Genome editing in primary cells and *in vivo* using viral-derived nanoblades loaded with Cas9-sgRNA ribonucleoproteins. *Nat. Commun.* 10 (1), 45. doi: 10.1038/s41467-018-07845-z
- Meyer, C., Losacco, J., Stickney, Z., Li, L., Marriott, G., and Lu, B. (2017). Pseudotyping exosomes for enhanced protein delivery in mammalian cells. *Int. J. Nanomed.* 12, 3153–3170. doi: 10.2147/IJN.S133430
- Montagna, C., Petris, G., Casini, A., Maule, G., Franceschini, G. M., Zanella, I., et al. (2018). VSV-g-enveloped vesicles for traceless delivery of CRISPR-Cas9. *Mol. Ther. Nucleic Acids* 12, 453–462. doi: 10.1016/j.omtn.2018.05.010
- Park, J., Bae, S., and Kim, J. S. (2015). Cas-designer: a web-based tool for choice of CRISPR-Cas9 target sites. *Bioinformatics* 31 (24), 4014–4016. doi: 10.1093/bioinformatics/btv537
- Pfaffl, M. W. (2001). A new mathematical model for relative quantification in real-time RT-PCR. *Nucleic Acids Res.* 29 (9), e45. doi: 10.1093/nar/29.9.e45
- Putyrski, M., and Schultz, C. (2012). Protein translocation as a tool: The current rapamycin story. *FEBS Lett.* 586 (15), 2097–2105. doi: 10.1016/j.febslet.2012.04.061
- Quinzo, M. J., Perteguer, M. J., Brindley, P. J., Loukas, A., and Sotillo, J. (2022). Transgenesis in parasitic helminths: a brief history and prospects for the future. *Parasit. Vectors* 15 (1), 110. doi: 10.1186/s13071-022-05211-z
- Sankaranarayanan, G., Coghlan, A., Driguez, P., Lotkowska, M. E., Sanders, M., Holroyd, N., et al. (2020). Large CRISPR-cas-induced deletions in the oxamniquine resistance locus of the human parasite *Schistosoma mansoni*. *Wellcome Open Res.* 5, 178. doi: 10.12688/wellcomeopenres.16031.1
- Schafer, P., Cymerman, I. A., Bujnicki, J. M., and Meiss, G. (2007). Human lysosomal DNase IIalpha contains two requisite PLD-signature (HxK) motifs: evidence for a pseudodimeric structure of the active enzyme species. *Protein Sci.* 16 (1), 82–91. doi: 10.1110/ps.062535307
- Selkirk, M. E., Huang, S. C., Knox, D. P., and Britton, C. (2012). The development of RNA interference (RNAi) in gastrointestinal nematodes. *Parasitology* 139 (5), 605–612. doi: 10.1017/S0031182011002332
- Sotillo, J., Sanchez-Flores, A., Cantacessi, C., Harcus, Y., Pickering, D., Bouchery, T., et al. (2014). Secreted proteomes of different developmental stages of the gastrointestinal nematode *Nippostrongylus brasiliensis*. *Mol. Cell Proteomics* 13 (10), 2736–2751. doi: 10.1074/mcp.M114.038950
- Vakulskas, C. A., and Behlke, M. A. (2019). Evaluation and reduction of CRISPR off-target cleavage events. *Nucleic Acid Ther.* 29 (4), 167–174. doi: 10.1089/nat.2019.0790
- van Schendel, R., Roerink, S. F., Portegijs, V., van den Heuvel, S., and Tijsterman, M. (2015). Polymerase theta is a key driver of genome evolution and of CRISPR/Cas9-mediated mutagenesis. *Nat. Commun.* 6, 7394. doi: 10.1038/ncomms8394
- Wu, Y. C., Stanfield, G. M., and Horvitz, H. R. (2000). NUC-1, a *Caenorhabditis elegans* DNase II homolog, functions in an intermediate step of DNA degradation during apoptosis. *Genes Dev.* 14 (5), 536–548. doi: 10.1101/gad.14.5.536